KKU Res. J. 2012; 17(2):203-210
http : resjournal.kku.ac.th

Influence of Annealing on the Giant Dielectric Properties of CuO Ceramics Prepared by a Simple PVA Sol–Gel

Thanin Putjuso and Peerasak Sangarun*

School of General Science, Faculty of Liberal Arts, Rajamangala University of Technology Rattanakosin, Wang Klai Kangwon Campus, 77110, Thailand
**Correspondent author: putjuso@hotmail.com*

Received January 6,2012
Accepted March 20,2012

Abstract

In this research, the giant dielectric constant CuO ceramics were successfully prepared by a simple PVA sol-gel method. Phase composition and microstructure were characterized by X-ray diffraction and scanning electron microscopy, respectively. The electrical and dielectric properties of the prepared CuO samples were investigated as functions of frequency (10^3 to 6.3×10^6 Hz) and temperature (-50 to 80 °C). The XRD results revealed that only the pure phase of CuO was obtained with the crystallite sizes of 21.93±6.53 nm. The sintered CuO ceramics exhibited a giant dielectric response ($\varepsilon' \sim 10^4$) with weak temperature dependence over the measured temperature. Interestingly, it was found that the giant dielectric constant of the CuO ceramic at low frequency was reduced by annealing in Ar, and could be enhanced up to the initial value by annealing in O_2. The reversibility of the dielectric constant can be explained by the interfacial polarization at the sample-electrode interface and at the outmost surface layer-inner part interface, resulting from a non-Ohmic contact

Keywords: Giant dielectric, Dielectric loss tangent, Copper oxide, SEM and XRD

1. Introduction

Recently, giant dielectric materials, dielectric constant (ε') of about ~10^4-10^6, have been attracted much attention due to their potential applications in the microelectronic industry. $CaCu_3Ti_4O_{12}$ (1-2), $Li_xTi_yNi_{1-x-y}O$ (3-4), $A(Fe_{1/2}B_{1/2})O_3$ (A=Ba, Sr, Ca and B=Nb, Ta, Sb) (5), and CuO (6-7) ceramics are included in the group of so-call "giant dielectric material". It was reported that the electrically heterogeneous structure, i.e., semiconducting grain and insulating grain boundary (GB), can be observed in these materials (8-9). Thus, it is widely accepted that the origin of the giant-ε' properties in these materials is associated with internal barrier layer capacitance (IBLC) effect, based on the interfacial polarization (Maxwell-Wagner polarization) at the GB (10) and/or electrodes (11). However, the complete explanation of such a giant-ε' behavior in these materials is still missing. All of these giant-ε' materials are of great interest because they are lead free and environment benign. Among of them, CuO ceramic shows a greatest motivation due to its low cost and simple compound. Moreover, CuO can be easily prepared in the pure form and it is commercially available on a large scale.

In this paper, we fabricated CuO ceramics from the fine CuO powder prepared by a simple polyvinyl alcohol sol-gel method. The dielectric properties of the sintered CuO ceramics were investigated as functions of temperature and frequency using impedance gain phase analyzer. Phase and microstructure of samples were characterized by XRD and SEM, respectively. Influence annealing on dielectric properties were performed in ultrahigh purity Ar (99.99%) and high purity O_2 (99.98%).

2. Materials and Methods

2.1 Powders preparation

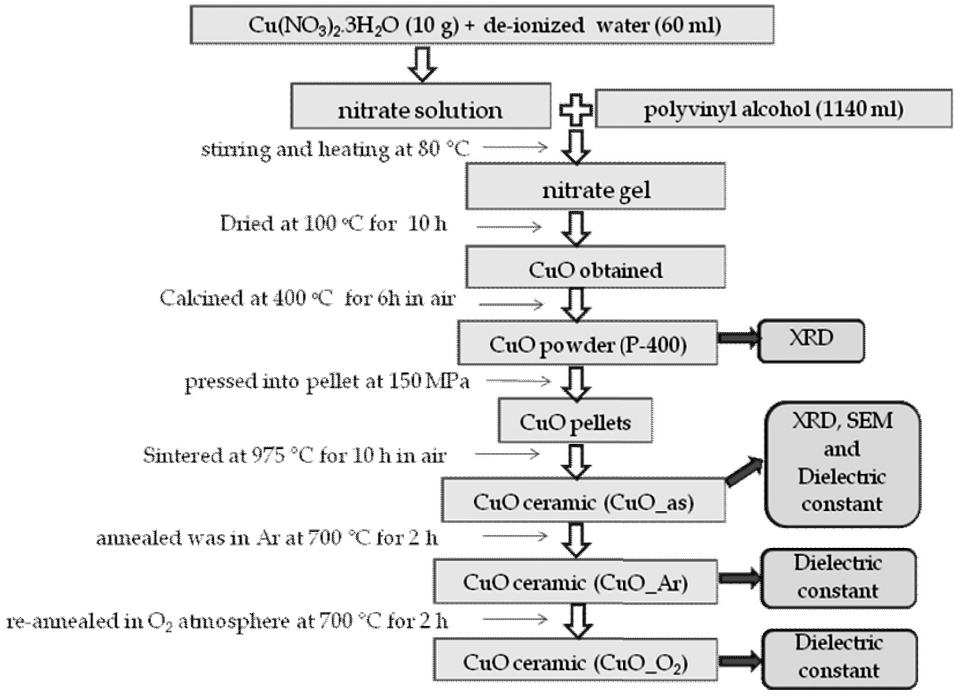

Figure 1. Diagram for the preparation of CuO powder by a Simple PVA Sol-Gel

In this work, copper nitrate ($Cu(NO_3)_2.3H_2O$) was employed as a starting material. The polycrystalline CuO powder was prepared by a simple polyvinyl alcohol (PVA) sol-gel method. In this experiment, 10 g of ($Cu(NO_3)_2.3H_2O$) was dissolved in 60 ml of de-ionized water under vigorous stir at room temperature (27 °C) until homogeneous solution was obtained. The nitrate solution was then mixed in 1140 ml of 5 wt% polyvinyl alcohol (Mn = 72,000, Fluka) aqueous solution by the ratio of 1:4 with stirring and heating at 80 °C until a viscous gel was formed. The gel was dried at 100 °C in air and ground to fine powder. This powder was calcined at 400 °C (indexed as P-400) in air for 6 h. The calcined powder was ball- milled (50 r/min) in a sealed alumina pot using zirconia balls under ambient condition for 5 h.

2.2 Ceramics preparation

In order to prepare the CuO ceramic, the obtained ball-milled powder was pressed into pellet each of 15 mm in diameter and ~ 1-2 mm in thickness by uniaxial pressing method at 150 MPa. These pellets were sintered at 975 °C in a box furnace for 10 h in air with the heating/cooling rate of 5 °C/min. The obtained pellets were black and called as-sample, denoted by CuO_as.

2.3 Samples characterizations

The phase and microstructure of CuO powders and ceramics were characterized by X-ray diffraction (XRD) (PW3040 Philips X-Pert MPD Multi Purpose CuKα radiation (l = 0.15406 nm), The Netherlands), and scanning electron microscopy (SEM) (LEO SEM VP1450, UK), respectively. Both surfaces of each pellet of as-sample (CuO_as) were polished, cleaned, dried and electroded by painting the silver paste on. They were allowed to dry overnight. The dielectric response of each sample was measured using a Hewlett Packard 4194A impedance gain phase analyzer over a frequency range of 100 Hz and 1 MHz at an oscillation voltage of 1.0 V. The measurements were performed in the temperature range of -50 and 120 °C using a built-in cooling-heating system. In each measurement, temperature was kept constant with in an accuracy of ± 1 °C.

2.4 Samples annealing

In order to study the annealing effect, another pellet from the same batch was used. This pellet was heated twice. First, it was annealed in Ar at 700 °C for 2 h, denoted as CuO_Ar. After annealing, it was immediately electroded without surface polishing and keeping dry further for dielectric measurement. After the dielectric measurement, the surface of CuO_Ar sample was polished in order to get rid of the electrodes and it was further re-annealed in O_2 atmosphere at 700 °C for 2 h, denoted as CuO_O_2. This CuO_O_2 was re-electroded and the dielectric was re-measured.

2.5 Data Analysis

The complex permittivity e^* was calculated as follows

$$\varepsilon^* = \varepsilon' - j\varepsilon'' \quad (1)$$

and

$$\varepsilon' = \frac{C_p d}{\varepsilon_o A} \quad (2)$$

$$\varepsilon'' = \varepsilon' \times \tan\delta \quad (3)$$

where C_p is the measured capacitance of the samples, ε_o is the permittivity in free space, A is the surface area of the sample, d is the sample thickness, ε'' is loss factor and $\tan\delta$ is dissipation factor.

3. Results and Discussion

3.1 XRD and SEM Results

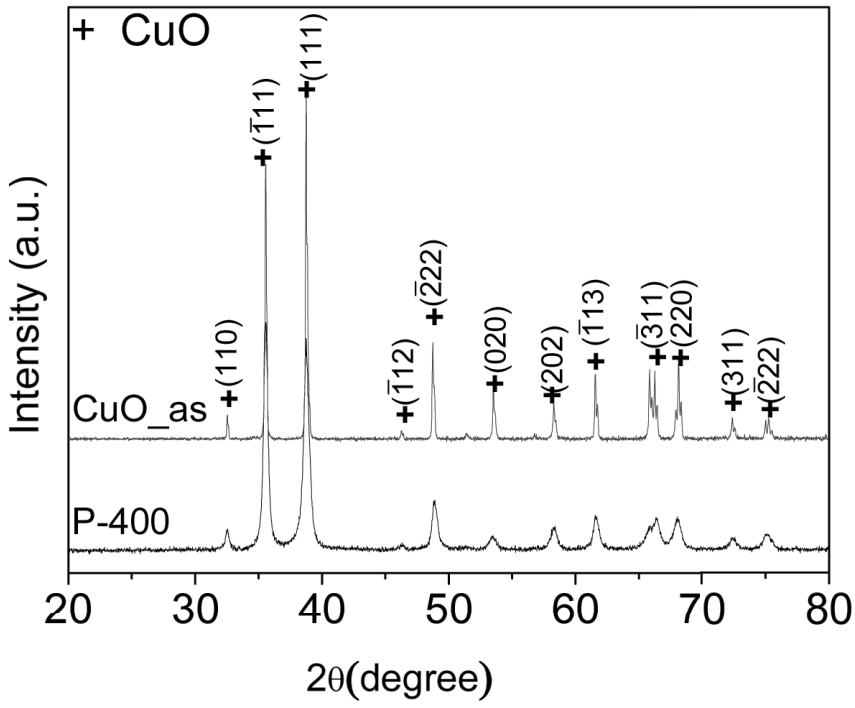

Figure 2. XRD patterns of CuO powder (P-400) and CuO_as ceramic .

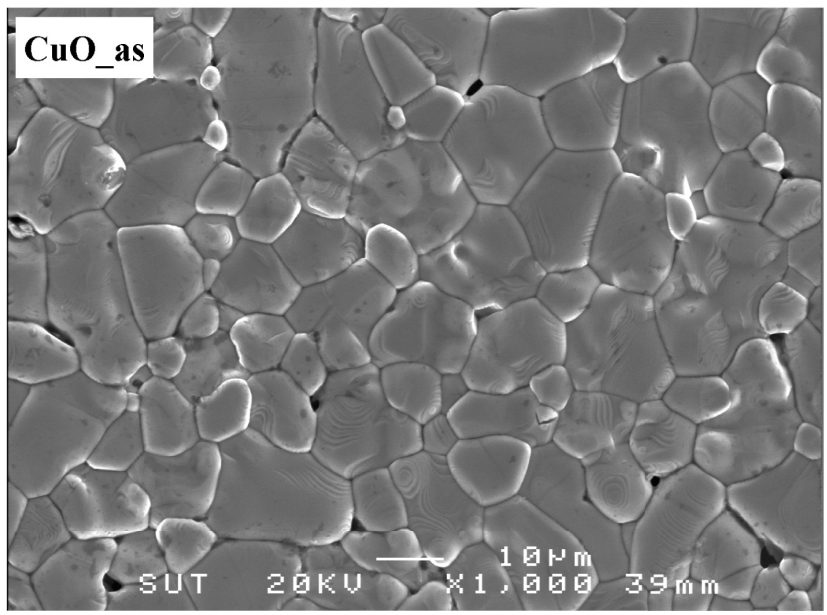

Figure 3. SEM micrograph of CuO_as ceramic.

Fig. 2 shows XRD patterns of the P-400 and CuO_as samples. It is clearly seen from figure 1 that both samples show a single phase of CuO (JCPDS card No.05-0661). From the X-ray line broadening of the reflection planes $(110),(\bar{1}11),(111),(\bar{2}22),(020),(202),(\bar{1}13),(\bar{3}11),(220),(311)$ and (222) the crystallite size (D) was estimated using the Scherrer formula (12),

$$D = \frac{K\lambda}{\beta\cos\theta} \quad (4)$$

where λe is the wavelength of the X-ray radiation, K is a constant taken as 0.975, θ is the diffraction angle and β is the full width at half maximum (FWHM) (by using program profile fit 1.0) which is given by $\beta=(\beta_o^2-\beta_i^2)^{1/2}$, where β_o and β_i are the widths of the observed X-ray peak and the width due to instrumental effects, respectively. From this calculation, the crystallite size was found to be 22 ± 7 nm for the P-400 powder. Fig. 3 reveals the surface morphology of the CuO_as ceramic by SEM. It is obviously seen that the ceramic sample shows grain (G) and grain boundary (GB) structures with the average grain size of 14±4 mm.

3.2 Dielectric Results

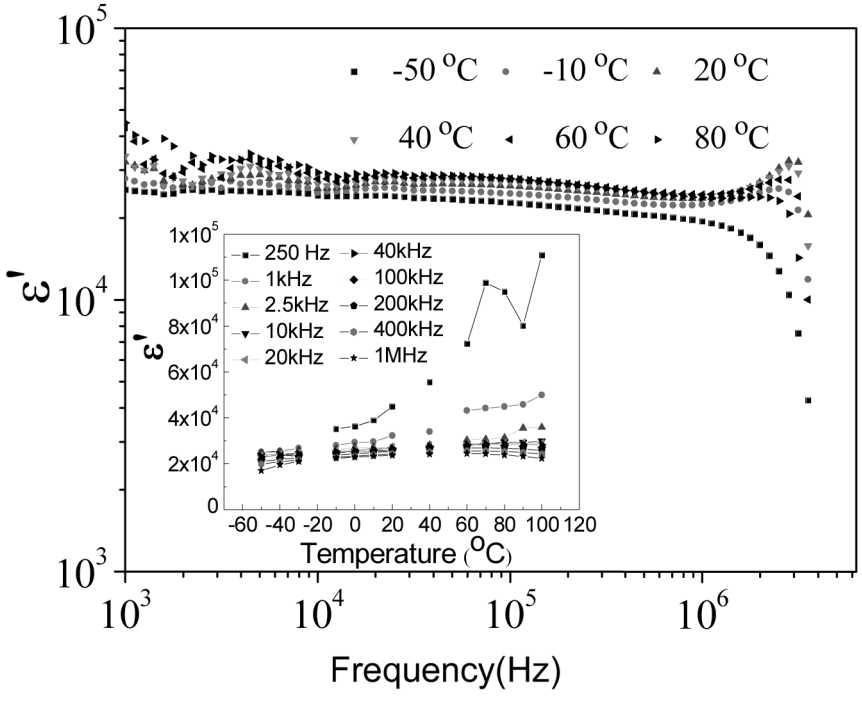

Figure 4. Frequency dependence of the dielectric constant at different temperature for the CuO_as sample. Inset is the temperature dependence of the dielectric constant at different frequency.

Fig. 4 illustrates the frequency and the temperature (inset) dependence of the giant dielectric of the CuO_as sample in the temperature range of -50 to 80 °C. The giant dielectric of the CuO_as samples is nearly frequency independent in the frequency range of 10^3 to 6.3×10^6 Hz. Moreover, the inset of Fig. 4 shows the temperature independence of the giant dielectric from -50 to 100 °C in the frequency range of 10^3 to 10^6 Hz. The overall dielectric behavior of the CuO_as ceramics prepared by a simple PVA sol-gel method is similar to those observed in the CuO ceramics prepared by high purity CuO powder (13).

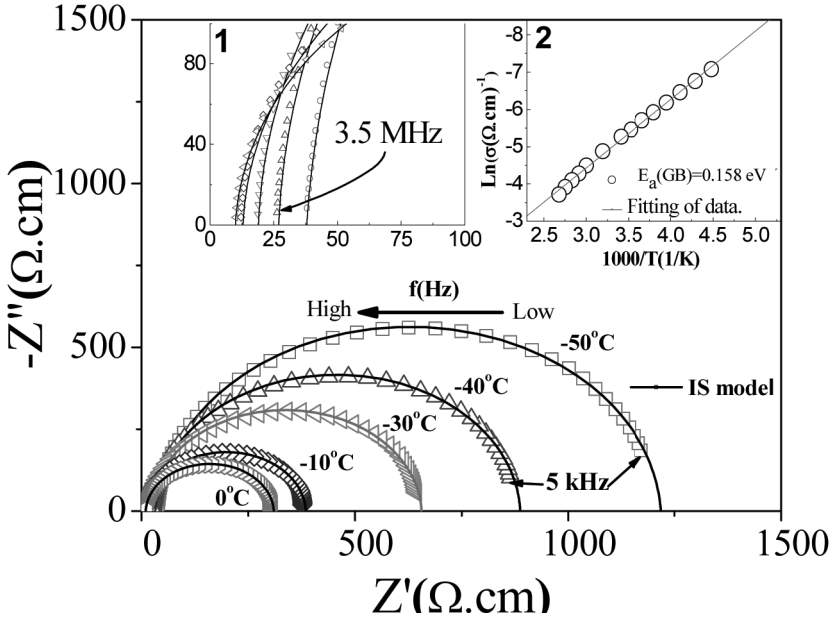

Figure 5. Complex impedance, Z* plots ($Z^{/}$ and $Z^{//}$); inset 1 shows non zero intercept at a high frequency and inset 2 reveals the Arrhenius plots of R_{ext} for the CuO_as samples.

Fig. 5 shows the complex impedance Z* plot of the CuO_as sample at various temperature from -50 to 0 °C. The observed two semicircular arcs indicate that there are at least two electrical responses in our CuO_as ceramics. According to the work reported by Li et al. (14), the large semicircle at low frequency can be assigned as the resistance of electrode, which refers to the external resistance (R_{ext}). The high-frequency electrical response can be assigned as the internal resistance (R_{int}) owing to the effects of grain and grain boundary. As illustrated in Fig. 5, with increasing temperature from -50 to 0 °C, the radius of the large semicircular arc is significantly decreased with the R_{ext} decreases, while the non zero intercept on the $Z^{/}$ axis at high frequency decrease from 37 to 26, 19 and 12 W.cm, respectively (inset 1). These results are similar to those observed in the CuO ceramics prepared by using the commercial CuO powder (13). The Arrhenius plot of Z* data and the R_{ext} (15) as shown in inset 2 provides an activation energy of the external effect (E_{ext}=0.158 eV), while the internal effect data can not be fitted. Thus, the IS analysis clearly demonstrates that the external effect is more resistive than the internal effect in CuO_as sample.

3.3 Annealing Results

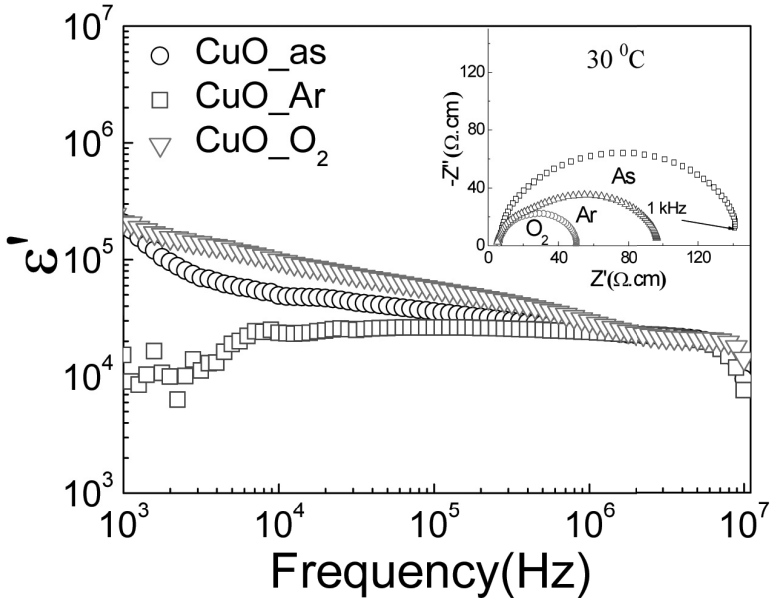

Figure 6. Frequency dependence of the dielectric constant of CuO_as, CuO_Ar and CuO_O_2 samples; inset shows the Complex impedance, Z* plots of these samples.

Fig. 6 shows the high dielectric constant of 206 000 at room temperature and 1 kHz in CuO_as sample. Interestingly, it was found that this value decreased to 15 200 after annealing in Ar (CuO_Ar sample) and it can be increased to around 210 666 after re-annealing in O_2 (CuO_O_2 sample), while the resistances (R_{ext}) were decreased (inset) from 125 to 90 and 40 W.cm in CuO_as, CuO_Ar and CuO_O_2 samples, respectively. The slightly decrease of R_{ext} in these samples might be due to the decrease of the samples' thickness, resulting from the polishing off the silver paint on their surfaces. These results strongly indicate that the oxygen vacancy has a great influence on the dielectric properties of the CuO ceramic. Based on the previous report (14), it can be suggested from our experimental data that the external effect depends on the concentration of oxygen vacancy at the surface of the CuO ceramic. This implies that the formation of Schottky barrier at both interface of the CuO ceramic and electrodes is not only related to the work function of metal electrode, but also on the surface state of the CuO ceramic due to the concentration of oxygen vacancy at the surface.

4. Conclusion

The effect of annealing on the electrical responses of the electrode and surface layer of the giant dielectric constant CuO ceramic was investigated. It was found that the giant dielectric of the CuO_as ceramic was decreased by annealing in Ar and could be enhanced up to around the initial value after re-annealing in O_2. These indicated that the concentration of oxygen vacancy had an influence on the giant dielectric properties of the CuO ceramic. The external resistance of dielectric relaxations

was observed in the CuO_O_2 sample, which might be assigned as the outmost surface-layer, electrode-sample interface, and GB effects. The giant low-frequency dielectric response in the CuO ceramic was associated with the effects of electrode and the outmost surface-layer.

5. Acknowledgement

The authors would like to thank Rajamangala University of Technology Rattanakosin for financial support, the Center for Scientific and Technological Equipment, Suranaree University of Technology for providing SEM facilities, and The National Metals and Materials Technology Center (MTEC), Thailand Science Park, Pathumthani, 12120, Thailand for dielectric measurement.

6. References

(1) Subramanian MA, Dong L, Duan N, Reisner BA, Sleight AW. High Dielectric Constant in $ACu_3Ti_4O_{12}$ and $ACu_3Ti_3FeO_{12}$ Phases. J Solid State Chem. 2000; 151: 323–325.

(2) Ramirez AP, Subramanian MA, Gardel M, Blumberg G, Li D, Vogt T, et al. Giant dielectric constant response in a copper-titanate. Solid State Commun. 2000; 115: 217-220.

(3) Wu J, Nan CW, Lin Y, Deng Y. Giant Dielectric Permittivity Observed in Li and Ti Doped NiO. Phys Rev Lett. 2002; 89: 217601.

(4) Thongbai P, Yamwong T, Maensiri S. The sintering temperature effects on the electrical and dielectric properties of $Li_{0.05}Ti_{0.02}Ni_{0.93}O$ ceramics prepared by a direct thermal decomposition method. J Appl Phys. 2008; 104: 074109.

(5) Raevski IP, Prosandeev SA, Bogatin AS, Malitskaya MA, Jastrabik L. High dielectric permittivity in $AFe_{1/2}B_{1/2}O_3$ nonferroelectric perovskite ceramics (A=Ba, Sr, Ca; B=Nb, Ta, Sb). J Appl Phys. 2003; 93: 4130.

(6) Sarkar S, Jana PK, Chaudhuri BK, Sakata H. Copper (II) oxide as a giant dielectric material. Appl Phys Lett. 2006; 89: 212905.

(7) Sarkar S, Jana PK, Chaudhuri BK. Colossal internal barrier layer capacitance effect in polycrystalline copper (II) oxide. Appl Phys Lett. 2008; 92: 022905.

(8) Sinclair DC, Adams TB, Morrison FD, West AR. One-step internal barrier layer capacitor. Appl Phys Lett. 2002; 80: 2153.

(9) Lin Y, Li M, Nan C, Li J, Wu J, He J. Grain and grain boundary effects in high-permittivity dielectric NiO-based ceramics. Appl Phys Lett. 2006; 89: 032907.

(10) Liu J, Duan C, Mei WN, Smith RW, Hardy JR. Dielectric properties and Maxwell-Wagner relaxation of compounds *A*Cu3Ti4O12 (*A*=Ca,$Bi_{2/3}$,$Y_{2/3}$,$La_{2/3}$). J Appl Phys. 2005; 98: 093703.

(11) Lunkenheimer P, Fichtl R, Ebbinghaus SG, Loidl A. Nonintrinsic origin of the colossal dielectric constants in $CaCu_3Ti_4O_{12}$. Phys Rev B. 2004; 70: 72102.

(12) Cullity BD, Stock SR. Elements of X-ray Diffraction. Prentice Hall: Englewood Cliffs; 2001.

(13) Thongbai P, Maensiri S, Yamwong T. Effects of grain, grain boundary, and dc electric field on giant dielectric response in high purity CuO ceramics. J Appl Phys. 2008; 104: 036107.

(14) Li M, Feteira A, Sinclair DC. Relaxor ferroelectric -like high effective permittivity in leaky dielectrics/oxide semiconductors induced by electrode effects: A case study of CuO ceramics. J Appl Phys. 2009; 104: 114109.

(15) Mott NF, Davis EA. Electronic Processes in Non-crystalline Materials. Clarendon: Oxford; 1979.